

Article

A Novel MPPT Technique Based on Combination between the Incremental Conductance and Hysteresis Control Applied in a Standalone PV System

Hind El Ouardi ¹, Ayoub El Gadari ¹, Mohcine Mokhlis ², Youssef Ounejjar ^{1,*}, Lahcen Bejjit ¹ and Kamal Al-Haddad ³

¹ Electrical Engineering Department, High School of Technologie (EST), University Moulay Ismail, Meknes 50000, Morocco

² Electrical Engineering Department, Mohammed V University, Rabat 10000, Morocco

³ Electrical Engineering Department, Ecole de Technologie Supérieure (ETS), Montreal, QC 11290, Canada

* Correspondence: ounejjar@gmail.com

Abstract: A new Maximum Power Point Tracking (MPPT) method, consisting in combining the Incremental Conductance (INC) algorithm with the Hysteresis control, was developed and applied to a standalone photovoltaic (PV) system to generate the maximum power of the PV array. The INC allows one to search for the Maximum Power Point (MPP). The hysteresis improves the accuracy of tracking the MPP very fast even after severe changes in weather conditions and has no oscillations around the MPP. The five-level S-Packed U Cells (SPUC5) inverter is used to transform the produced DC voltage to AC voltage; it generates five-level output voltage with a small number of switches and only DC source voltage. The capacitors of the SPUC5 are controlled by the Pulse Width Modulation (PWM) in order to balance their voltages. The proposed PV system was established and trained in the MATLAB/Simulink environment under various irradiation conditions. A comparison between different MPPT methods, INC-PWM and INC-PI, was investigated in order to examine the effectiveness of the developed MPPT technique in particular, and of all the PV system components. The results of the simulation validate the effectiveness of the suggested MPPT algorithm as well as the used SPUC5 inverter.



Citation: El Ouardi, H.; El Gadari, A.; Mokhlis, M.; Ounejjar, Y.; Bejjit, L.; Al-Haddad, K. A Novel MPPT Technique Based on Combination between the Incremental Conductance and Hysteresis Control Applied in a Standalone PV System. *Eng* **2023**, *4*, 964–976. <https://doi.org/10.3390/eng4010057>

Academic Editor: Jingzheng Ren

Received: 31 December 2022

Revised: 27 February 2023

Accepted: 28 February 2023

Published: 12 March 2023



Copyright: © 2023 by the authors. Licensee MDPI, Basel, Switzerland. This article is an open access article distributed under the terms and conditions of the Creative Commons Attribution (CC BY) license (<https://creativecommons.org/licenses/by/4.0/>).

Keywords: hysteresis band; incremental conductance; MPPT; multilevel inverter; PWM; SPUC5; total harmonic distortion (THD)

1. Introduction

The global request for electrical energy in the world is growing daily as the standard of living improves, while the stock of fossil fuels is decreasing. It is one of the many problems caused by fossil energies that have prompted the world to seek and invest in alternative energy sources [1]. Solar, wind and hydraulic energy are the most common inexhaustible and dependable energy sources. Solar energy has several applications, including heat supply via thermodynamic solar systems [2], hot water production via solar water heaters [3] and electricity generation via PV systems [4].

The function of PV systems is to absorb sunlight and convert it into electricity through the PV cells [5]. It is the most practical clean technology due to its operational nature and simplicity. However, there are some problems associated with these systems in terms of their efficiency: the operating point of the PV panel shifts from open to short-circuit conditions. Thus, in order to operate at the MPP, an MPPT controller is usually required. Different algorithms have been developed and implemented by researchers in this context. Among these algorithms, we note Perturb and Observe (P&O) [6,7]. Its principle consists in disturbing the voltage of the PV array and comparing the instantaneous power with that of the previous disturbance. Then, the direction of the disturbance depends on the increase or decrease in power. Incremental conductance (INC) [8,9] utilizes the slope of the P-V curve

of the PV array characteristics to determine the MPP. This slope is equal to zero at the MPP, positive to its left and negative to its right. The process of Fuzzy Logic (FL) control [10] consists in taking an input value and making it undergo a fuzzification (first step); then, it is treated by an inference engine (second step), and lastly, it undergoes a defuzzification stage.

In PV systems, the presence of an inverter is also mandatory to switch the DC voltage at the exit of the converter into an AC voltage to supply the alternating load or grid. Multilevel inverters have many advantages compared to two-level inverters. They produce a reduced total harmonic distortion (THD) with a low switching frequency and an optimized output voltage. Over the years, a variety of multilevel inverter topologies have been developed. Citing the classical ones, such as Neutral Point Clamped (NPC) [11,12], Flying Capacitor (FC) [13,14] and Cascaded H-bridge (CHB) [15], these inverters use a large number of components and even more than one DC source. For those reasons, researchers have developed new topologies of multilevel inverters such as Packed U-Cells (PUC) [16–18], which needs a low number of passive and active switches and provides a high number of levels without using filters or sensors, and Split Packed U-Cells (SPUC) [19], which is able to combine capacitors together, and also uses a small number of components with an uncomplicated PWM control technique. The SPUC inverter is very competitive in PV systems in standalone mode [20,21], as well as in grid-connected mode as published in [22,23].

In this work, a new MPPT controller based on the Hysteresis technique has been proposed to control the boost converter DC/DC in order to achieve the MPP of the PV array. The five-level SPUC inverter DC/AC has been chosen in this paper with a PWM controller to supply the load with a high-quality AC voltage. The presented standalone PV system has been tested and simulated under Standard Test Conditions (STC) and under different irradiation conditions to evaluate the performance of the proposed technique.

The rest of the document is organized as follows: Section 2 explains the proposed MPPT algorithm, Section 3 is dedicated to the description of the components of the proposed PV system, Section 4 discusses simulation results, and Section 5 is dedicated to the conclusion.

2. The Proposed MPPT Technique Based on the Hysteresis Control

The INC algorithm is among the most popular techniques used for MPPT of PV systems. It has a simple process of tracking and does not require a large amount of memory space for implementation. The MPP is tracked by detecting the slope of the P-V curve of the PV panel and then searching for the peak of this curve. The MPP is only reached when its value is equal to zero, as shown in Equation (1):

$$\frac{dP}{dV} = 0, \quad (1)$$

where dP is the variation of the output power of the PV panel and dV is the variation of the output voltage of the PV panel.

The INC algorithm calculates the instantaneous conductance I/V and the incremental conductance dI/dV to determine the MPP. By deriving Equation (1), the following equations are obtained:

$$\left\{ \begin{array}{l} \frac{dI}{dV} = -\frac{I}{V} \\ \frac{dI}{dV} > -\frac{I}{V} \\ \frac{dI}{dV} < -\frac{I}{V} \end{array} \right. \quad (2)$$

$$\left\{ \begin{array}{l} \frac{dI}{dV} > -\frac{I}{V} \\ \frac{dI}{dV} < -\frac{I}{V} \end{array} \right. \quad (3)$$

$$\left\{ \begin{array}{l} \frac{dI}{dV} < -\frac{I}{V} \end{array} \right. \quad (4)$$

The previous equations provide the three cases of the P-V curve: Equation (2) means that the PV panel is running at MPP, Equation (3) means that the PV panel is running to the left of MPP, and Equation (4) means that the PV panel is running to the right of the MPP.

However, this method has some drawbacks; it makes oscillations around MPP and has no regular adaptation. Therefore, it requires an auxiliary controller to enhance its efficiency.

PWM controller is added to the INC by authors in [20], which quickly tracks the MPP in a standalone PV system even under the change of irradiation, but the oscillations still appear. A Proportional Integral (PI) controller is adopted for the variable step INC algorithm in [24]; it can track the MPP faster and more precisely.

This work proposes to associate a Hysteresis Band controller to the INC. This combination ensures improved tracking performances either at the level of speed and accuracy or at the level of oscillation reduction.

In effect, as previously explained, the INC allows for the identification the MPP, after which the hysteresis improves the tracking accuracy and reduces oscillations around it.

The hysteresis has the advantage of controlling the voltage delivered by the INC block and not the duty cycle. The value of the measured voltage is directly compared to the reference voltage. The voltage error is then immediately compared to the hysteresis band to provide switching pulses for the boost converter.

This method is designed to control the switch of the boost converter to ramp the voltage up and down in order to follow the reference voltage signal.

The error is the difference between the generated voltage and the desired voltage. It is used for controlling the boost converter switch. The maximum and minimum values of the error signal form the Upper and Lower Hysteresis band, respectively, are shown in Figure 1.

$$\text{Upper Hysteresis Band} = V_{ref} + e_{max}, \quad (5)$$

$$\text{Lower Hysteresis Band} = V_{ref} - e_{min}, \quad (6)$$

where V_{ref} is the reference voltage, e_{max} presents the maximum value of the error, and e_{min} is the minimum value of the error signal.

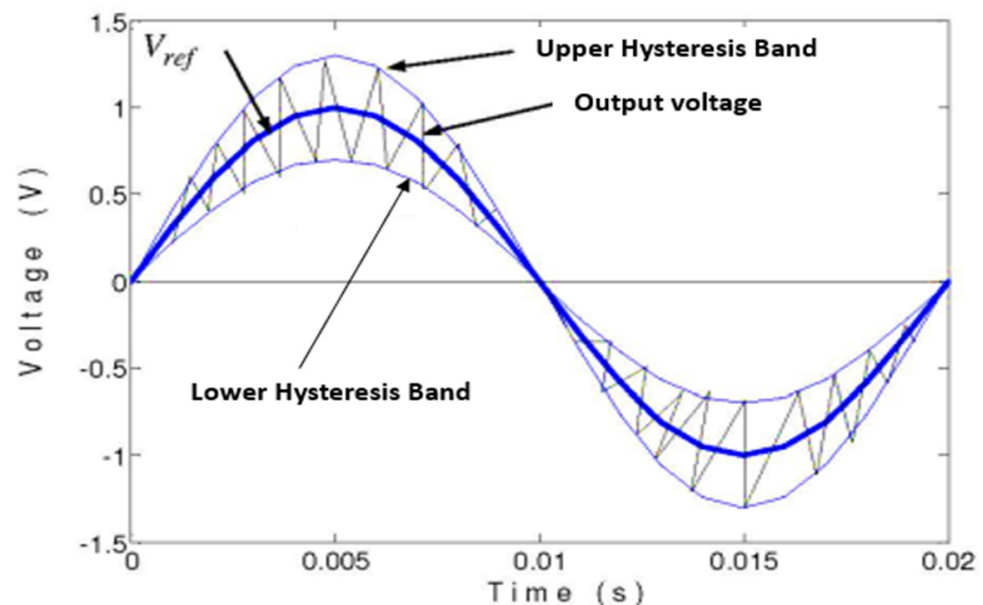


Figure 1. The Hysteresis voltage control principle.

The voltage must remain between the Upper and Lower Hysteresis Band. For this reason, when the real value of the voltage attains the Upper Hysteresis Band, the switch turns ON to enforce the voltage to decrease, and when it attains the Lower Hysteresis Band, the switch turns ON to enforce the voltage to increase.

3. The Studied Photovoltaic System

The components of the proposed PV system are presented and modeled in this section; the power is produced by a PV panel, connected to the boost converter in order to track the MPP and regulate the DC voltage. This component is connected to the SPUC5 inverter, which converts DC voltage into AC voltage in order to supply the load.

3.1. The PV Array

The PV panel is the source of the energy in every PV system. It is composed of several cells connected to each other. The general circuit of a PV cell is presented in Figure 2 [25].

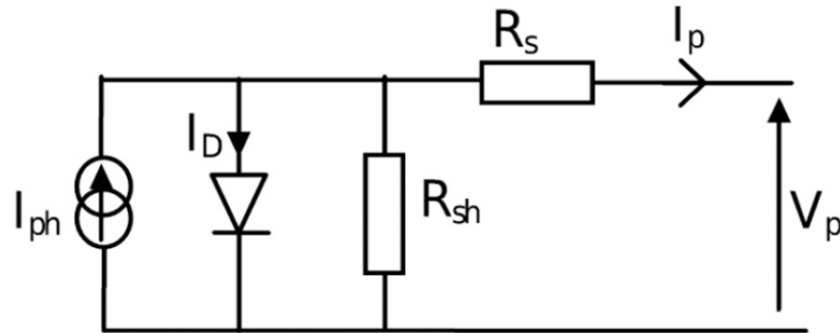


Figure 2. General circuit of a one-diode PV cell.

The mathematical equation of the current generated by a PV panel constituted of N number of cells is described as follows:

$$I_p = I_{ph} - I_s \left[\exp \left(\frac{q(V_p + R_s I_p)}{\gamma K T} \right) - 1 \right] - \frac{V_p + R_s I_p}{R_{sh}}, \tag{7}$$

where

$$I_{ph} = \left[I_{ph0} + K_i(T - T_{STC}) \right] \frac{G}{G_{STC}}, \tag{8}$$

$$I_s = I_{s0} \left(\frac{T}{T_{STC}} \right)^3 \exp \left[q \frac{E_G}{\gamma K} \left(\frac{1}{T_{STC}} - \frac{1}{T} \right) \right], \tag{9}$$

with I_{pV} as the current generated by the PV panel, I_{ph} presenting the photo-current, I_s as the diode saturation current, q as the electron charge ($q = 1.60217646 \times 10^{-19}$ C), V_p presenting the PV panel voltage, I_p as the PV panel current, R_s as the series resistance, γ as the ideality factor of the diode, K presenting the Boltzmann constant and its value as $1.3806503 \times 10^{-23}$ J/K, T as the temperature cell, R_{sh} presenting the parallel resistance, I_{ph0} presenting the photo current measured under STC ($G_{STC} = 1000$ W/m² and $T_{STC} = 25$ °C are, respectively, the irradiation and the temperature at STC), K_i as the temperature coefficient of short circuit current, G as the irradiation, I_{s0} as the saturation current under STC, T_{STC} and E_G presenting the band gap energy.

In this study, the authors chose SOLARIA S6M2G240 for reference of the PV module. The P-V curve of the latter under different irradiances is presented in Figure 3.

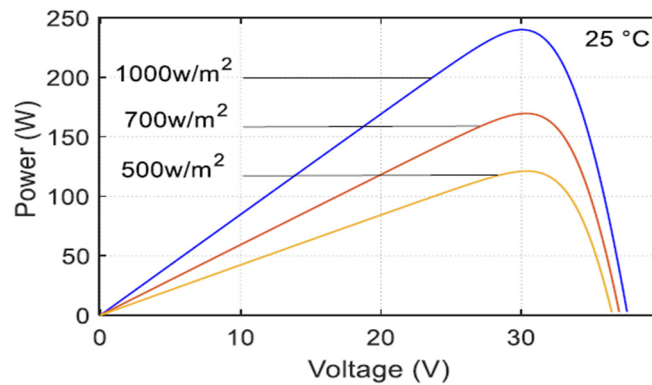


Figure 3. P-V curve of SOLARIA S6M2G240 module under different irradiance.

Table 1 lists the parameters of the chosen PV panel at the STC.

Table 1. SOLARIA S6M2G240 module parameters.

Parameters	Values
Maximum power P_{max} (W)	240
Optimum voltage at P_{max} (V)	30.05
Optimum current at P_{max} (A)	7.99
Open circuit voltage V_{oc} (V)	37.58
Short circuit current I_{sc} (A)	8.49
Series resistance (Ω)	0.3783
Parallel resistance (Ω)	639.7
Number of cells	60

3.2. DC/DC Boost Converter

A DC/DC conversion stage is needed in PV systems, after the PV array and before the inverter, in order to increase or decrease the DC voltage introduced by PV panels and to reach their maximum power point by controlling this converter with an MPPT controller [26].

In our system, the DC/DC converter is a boost converter, which allows increasing the input voltage V_i according to the following equation:

$$V_o = \frac{V_i}{1 - \alpha'} \tag{10}$$

where V_o presents the output voltage, and α is the duty cycle.

The used boost converter consists of a switch S , a diode D , an inductor L , and three Capacitors $C1$, $C2$ and $C3$ as shown in Figure 4.

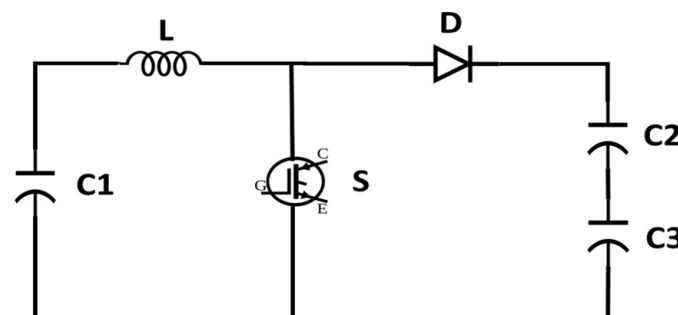


Figure 4. The used boost converter circuit.

3.3. SPUC5 Inverter

In order to supply the load with AC voltage, we need to use an inverter; the SPUC5 is the topology chosen due to its efficiency. It is based on the combination of the PUC and the NPC technologies, which permits it to benefit from the advantages of both. On the one hand, it generates five voltage levels with only five switches (T1, T2, T3, T4 and T5), one DC source (E) and two capacitors (C1 and C2). On the other hand, it provides the possibility to join capacitors together.

The capacitor voltages are properly balanced using the PWM technique without the need for any PI regulators or filters. Figure 5 shows the SPUC5 inverter scheme.

Before applying it to the proposed PV system, the SPUC5 inverter is verified with a constant 300 V DC source.

Table 2 shows the switching sequence of the SPUC5 inverter with the redundant state and the output voltage in each state. V_{C1} and V_{C2} are, respectively, the voltages of Capacitor 1 and Capacitor 2.

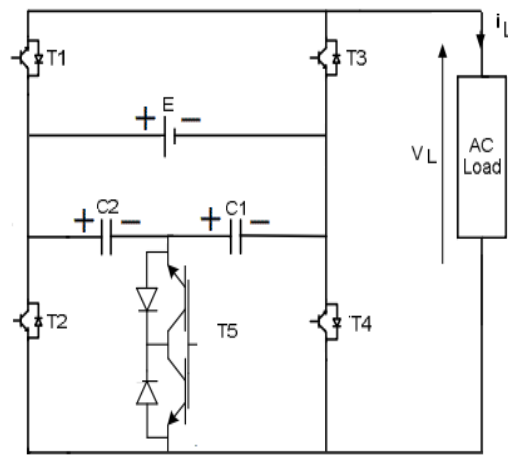


Figure 5. SPUC5 inverter scheme.

Table 2. SPUC5 inverter switching sequence.

State	Output Voltage (V)	Switch Pulses				
		T1	T2	T3	T4	T5
1	E	1	0	0	1	0
2	V_{C1}	1	0	0	0	1
3	0	0	0	1	1	0
4	$-V_{C1}$	0	0	1	0	1
5	-E	0	1	1	0	0

The output voltage is constituted of five levels: 300 V, 150 V, 0 V, -150 V and -300 V as shown in Figure 6. The THD of the load voltage is presented in Figure 7 (around 27.57%).

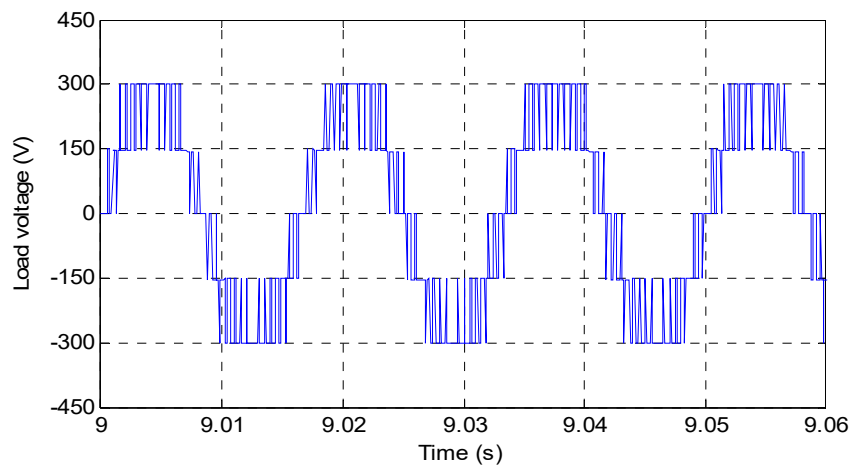


Figure 6. Load voltage waveform.

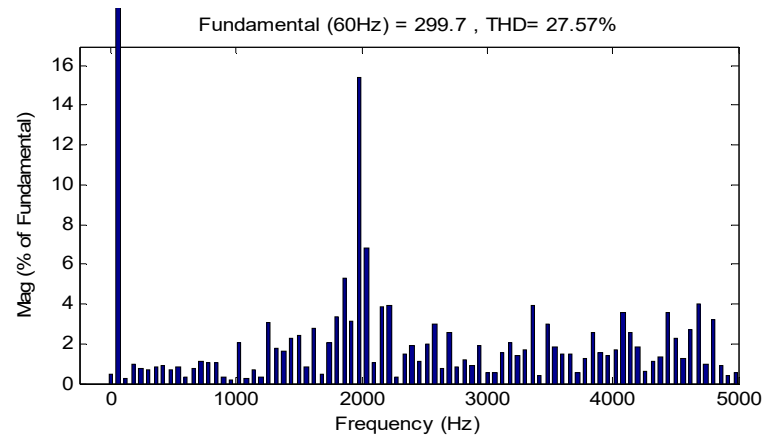


Figure 7. THD of the output voltage.

4. Simulation Results

The offered PV system has been modeled and simulated in the MATLAB/Simulink software under severe temperature and irradiation conditions, as shown in Figures 8 and 9, in order to demonstrate the efficiency of the proposed MPPT technique, in particular, and the entire studied PV system in general.

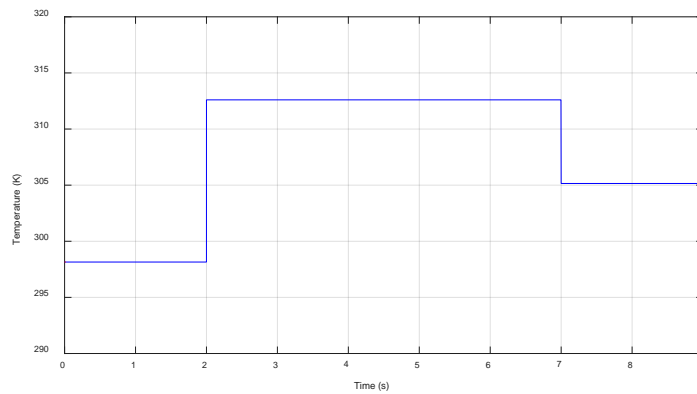


Figure 8. Temperature variation during simulation.

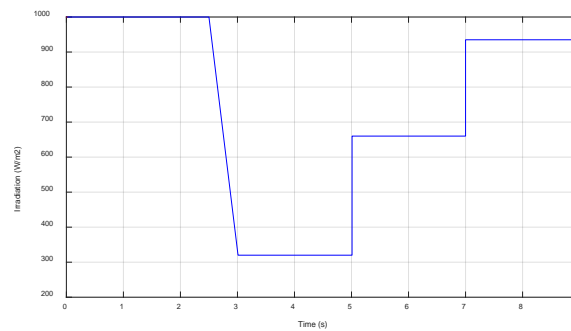


Figure 9. Irradiance variation during simulation.

At first [0,2 s], the PV panel is exposed to STC (1000 W/m² of irradiation and 25 °C of temperature), then the temperature was increased to attain 39 °C with the same irradiation until 2.5 s; thereafter, the irradiation underwent an orthogonal decrease to reach 320 W/m² at 3 s and remain stable until 5 s; after that, the irradiation suddenly changed to 660 W/m² from 5 s to 7 s; beyond this period, the simulation continued with a temperature of 32 °C and an irradiation of 935 W/m².

The parameters of the PV system during the simulation are listed in Table 3.

Table 3. Simulation parameters.

Parameters	Values
Switching frequency (KHz)	2
Load resistance (Ω)	5
Load inductor (H)	15
SPUC5 capacitors (μF)	4000

4.1. Simulation Results of the Proposed PV System

Figure 10 shows the output power of the PV panel using the INC-HYS algorithm; the MPP is reached after a short simulation time; it is approximately 240 W for 1000 W/m² and 25 °C of temperature, which is in accordance with the characteristics of the PV module presented in the datasheet Figure 3. As the temperature rises, the power decreases proportionally to the irradiation to reach approximately 70 W for 320 W/m² and 39 °C. In the irradiation of 660 W/m², the power decreases to quickly attain 150 W; after, in the last change in irradiancies and temperature (respectively, 935 W/m² and 32 °C), the PV panel power increases to 220 W. These remarks validate the effectiveness of the proposed INC-HYS technique to reach the MPP rapidly and accurately even under difficult changing weather conditions. The same occurs for the PV panel voltage, as illustrated in Figure 11, in the time interval of [0,2 s] under STC; the voltage value reaches 30 V after a short time, which is the value corresponding to the maximum power as shown in Figure 3, then the voltage changes and takes the optimal value for each weather condition.

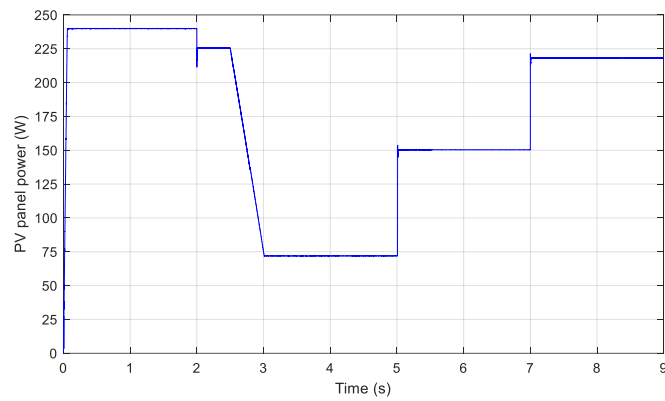


Figure 10. PV panel power.

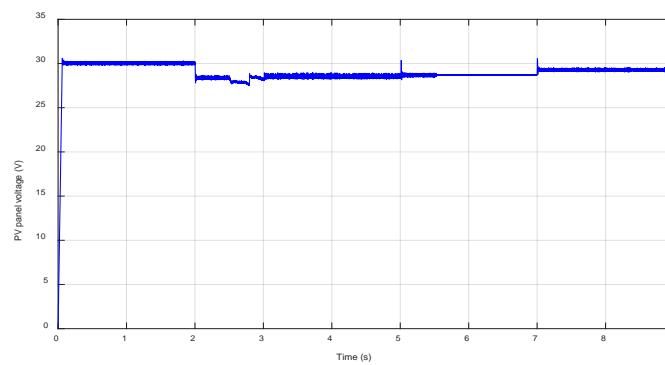


Figure 11. PV panel voltage.

The DC-link voltage is shown in Figure 12. It is well regulated and its values change according to the weather conditions. Figure 13 presents the SPUC5 capacitor voltages. They are properly controlled and maintained at half of the DC-link voltage.

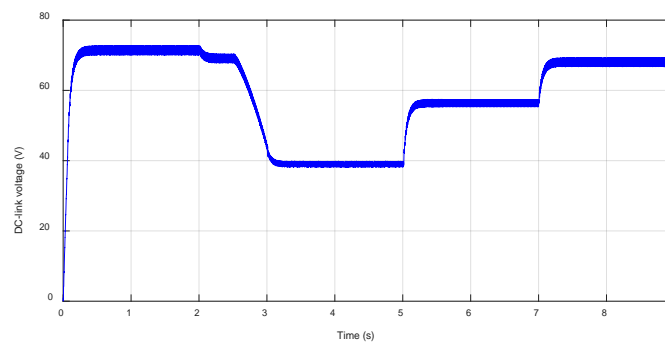


Figure 12. DC-link voltage.

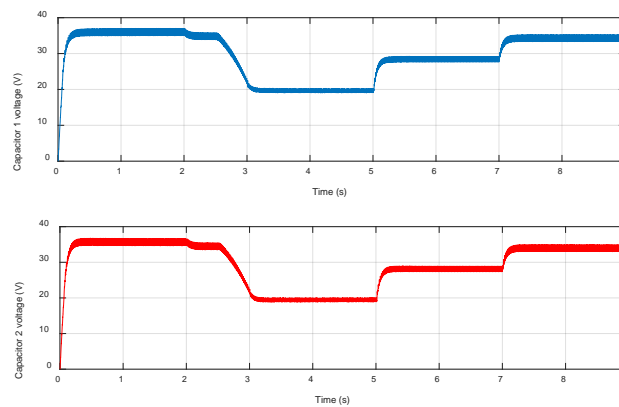


Figure 13. SPUC5 capacitor voltages.

The load voltage is illustrated in Figure 14. The voltage is comprised of five levels. Figure 15 shows the load current; the waveform is quasi-sinusoidal and its THD is approximately 1.05%, as shown in Figure 16, without using any filters, which ensures the efficiency of the used inverter and its controller.

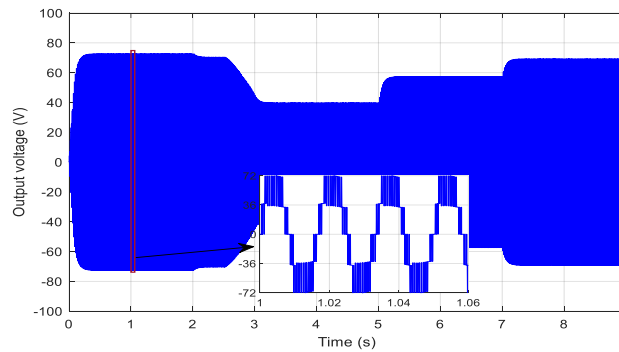


Figure 14. Output voltage.

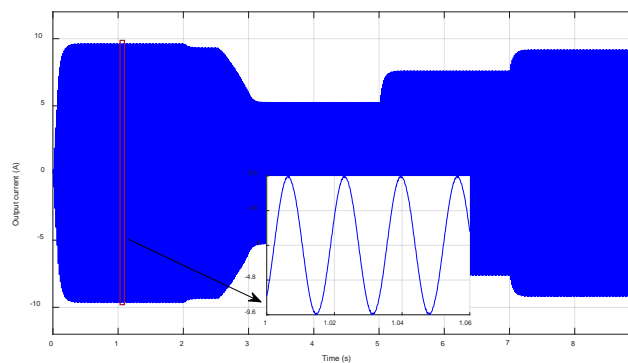


Figure 15. Output current.

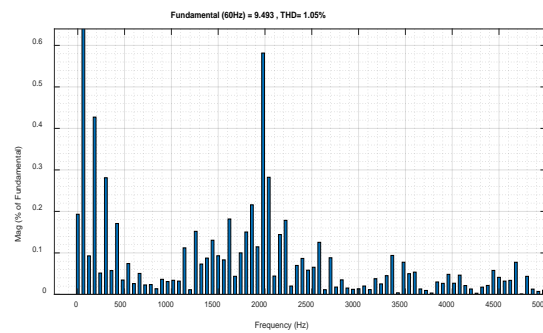


Figure 16. THD of the output current.

4.2. Comparative Study

A comparative study was conducted with the INC-PWM and INC-PI algorithms to better verify the performance of the proposed MPPT algorithm (INC-HYS).

Figure 17 shows the output power of the PV panel for the three commonly used methods. As can be seen, the proposed method is faster than the INC-PI and INC-PWM to detect the MPP even after any irradiation or temperature changes. In addition, the INC-HYS technique is more accurate and has fewer oscillations compared to other methods as it is easy to implement. As a result, the proposed INC-HYS method to control the PV panel power ensures quicker and more efficient responses.

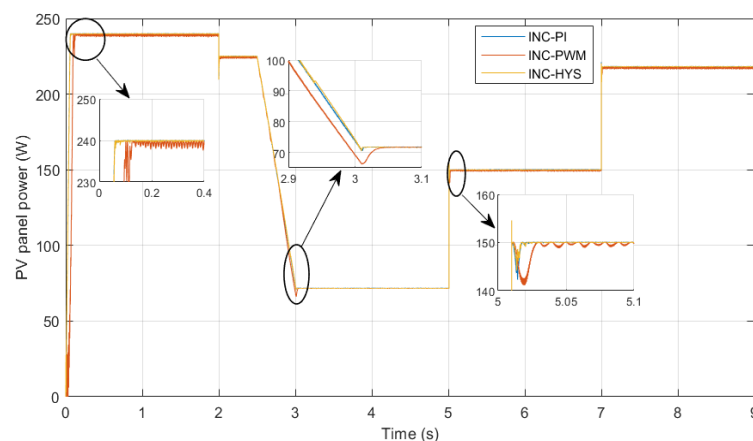


Figure 17. PV panel power comparison using INC-PI, INC-PWM and the proposed technique.

5. Conclusions

Simulations and comparison results have shown that the proposed combination of the Incremental Conductance and the Hysteresis provides high performance and good efficiency in terms of MPP tracking under static and dynamic weather conditions. The INC control is used to detect the MPP, whereas the Hysteresis control is proposed to minimize the oscillations around the MPP and improve the speed of detecting it. A boost DC/DC converter is also used to regulate and amplify the PV panel voltage.

The use of the new topology SPUC5 inverter, with PWM control technique to regulate the capacitor voltages, ensures a high signal quality to the load. The output voltage is composed of five levels and the current has a quasi-sinusoidal waveform with a 1.05% of THD without the need for any filters.

Thus, the proposed standalone PV system has provided good efficiency of all its components, from the panel to the load, whatever the external conditions.

Author Contributions: Conceptualization, H.E.O.; methodology, H.E.O. and M.M.; software, H.E.O.; validation, H.E.O. and Y.O.; formal analysis, H.E.O., M.M. and A.E.G.; writing—original draft preparation, H.E.O.; writing—review and editing, M.M. and Y.O.; visualization, H.E.O. and Y.O.; supervision, Y.O., K.A.-H. and L.B. All authors have read and agreed to the published version of the manuscript.

Funding: This research was funded by l'École de technologie supérieure (ETS), Montréal, Quebec, Canada.

Conflicts of Interest: The authors declare no conflict of interest.

References

1. Żywiołek, J.; Rosak-Szyrocka, J.; Khan, M.A.; Sharif, A. Trust in Renewable Energy as Part of Energy-Saving Knowledge. *Energies* **2022**, *15*, 1566. [[CrossRef](#)]
2. Shoeibi, S.; Kargarsharifabad, H.; Sadi, M.; Arabkoohsar, A.; Mirjalily, S.A.A. A review on using thermoelectric cooling, heating, and electricity generators in solar energy applications. *Sustain. Energy Technol. Assess.* **2022**, *52*, 102105. [[CrossRef](#)]
3. Barone, G.; Buonomano, A.; Palmieri, V.; Palombo, A. A prototypal high-vacuum integrated collector storage solar water heater: Experimentation, design, and optimization through a new in-house 3D dynamic simulation model. *Energy* **2022**, *238*, 122065. [[CrossRef](#)]
4. Abid, H.; Thakur, J.; Khatiwada, D.; Bauner, D. Energy storage integration with solar PV for increased electricity access: A case study of Burkina Faso. *Energy* **2021**, *230*, 120656. [[CrossRef](#)]
5. Verma, R.; Chauhan, A.; Kalia, R.; Jasrotia, R.; Sharma, M.; Kumar, R. A comprehensive study on piezo-phototronic effect for increasing efficiency of solar cells: A review. *Opt. Laser Technol.* **2022**, *149*, 107779. [[CrossRef](#)]
6. Khalf, D.; Hassan, K.; Shary, D. A PV generation system based on P&O MPPT algorithm and SVPWM inverter for standalone applications. In Proceedings of the 2nd International Multi-Disciplinary Conference Theme: Integrated Sciences and Technologies, IMDC-IST 2021, Sakarya, Turkey, 7–9 September 2021.
7. Rajamand, S. A novel sliding mode control and modified PSO-modified P&O algorithms for peak power control of PV. *ISA Trans.* **2022**, *130*, 533–552. [[PubMed](#)]
8. Pathak, P.K.; Padmanaban, S.; Yadav, A.K.; Alvi, P.A.; Khan, B. Modified incremental conductance MPPT algorithm for SPV-based grid-tied and stand-alone systems. *IET Gener. Transm. Distrib.* **2022**, *16*, 776–791. [[CrossRef](#)]
9. Mishra, J.; Das, S.; Kumar, D.; Pattnaik, M. A novel auto-tuned adaptive frequency and adaptive step-size incremental conductance MPPT algorithm for photovoltaic system. *Int. Trans. Electr. Energy Syst.* **2021**, *31*, e12813. [[CrossRef](#)]
10. Nasser, K.W.; Yaqoob, S.J.; Hassoun, Z.A. Improved dynamic performance of photovoltaic panel using fuzzy logic-MPPT algorithm. *Indones. J. Electr. Eng. Comput. Sci.* **2021**, *21*, 617–624. [[CrossRef](#)]
11. Jayakumar, V.; Chokkalingam, B.; Munda, J.L. A Comprehensive Review on Space Vector Modulation Techniques for Neutral Point Clamped Multi-Level Inverters. *IEEE Access* **2021**, *9*, 112104–112144. [[CrossRef](#)]
12. Beniwal, N.; Tafti, H.D.; Farivar, G.G.; Ceballos, S.; Pou, J.; Blaabjerg, F. A control strategy for dual-input neutral-point-clamped inverter-based grid-connected photovoltaic system. *IEEE Trans. Power Electron.* **2021**, *36*, 9743–9757. [[CrossRef](#)]
13. Sreejyothi, K.R.; Chenchireddy, K.; Lavanya, N.; Reddy, R.M.; Prasad, K.G.; Revanth, R. Level-Shifted PWM Techniques Applied to Flying Capacitor Multilevel Inverter. In Proceedings of the 2022 International Conference on Electronics and Renewable Systems (ICEARS), Tuticorin, India, 16–18 March 2022.
14. Hamida, M.L.; Fekik, A.; Denoun, H.; Ardjal, A.; Bokhtache, A.A. Flying Capacitor Inverter Integration in a Renewable Energy System. In *Modeling and Control of Static Converters for Hybrid Storage Systems*; IGI Global: Hershey, PA, USA, 2022; pp. 287–306.
15. Jayaprakash, S.; Balamurugan, R.; Gopinath, S.; Kokilavani, T.; Maheswaran, S. 3-Phase multi-inverter with cascaded H-bridge inverter designing and implementation for renewable system. *Sustain. Energy Technol. Assess.* **2022**, *52*, 102088. [[CrossRef](#)]
16. Abari, I.; Hamouda, M.; Sleiman, M.; Slama, J.B.H.; Kanaan, H.Y.; Al-Haddad, K. Open-Circuit Fault Detection and Isolation Method for Five-Level PUC Inverter Based on the Wavelet Packet Transform of the Radiated Magnetic Field. *IEEE Trans. Instrum. Meas.* **2022**, *71*, 1–11. [[CrossRef](#)]
17. Babaie, M.; Sharifzadeh, M.; Al-Haddad, K. Adaptive ANN based single PI controller for nine-level PUC inverter. In Proceedings of the 2019 IEEE Electrical Power and Energy Conference (EPEC), Montreal, QC, Canada, 16–18 October 2019.
18. Vahedi, H.; Sharifzadeh, M.; Al-Haddad, K. Modified seven-level pack U-cell inverter for photovoltaic applications. *IEEE J. Emerg. Sel. Top. Power Electron.* **2018**, *6*, 1508–1516. [[CrossRef](#)]
19. El Gadari, A.; El Ouardi, H.; Alibou, S.; Ounejjar, Y.; Bejjit, L.; Sharifzadeh, M.; Al-Haddad, K. New nine-level SPUC inverter using single DC source. In Proceedings of the IECON 2019—45th Annual Conference of the IEEE Industrial Electronics Society, Lisbon, Portugal, 14–17 October 2019; Volume 1.
20. El Ouardi, H.; El Gadari, A.; Ounejjar, Y.; Kamal, A.H.; Alibou, S. A standalone photovoltaic system based on the SPUC5 inverter. In Proceedings of the 2020 IEEE 29th International Symposium on Industrial Electronics (ISIE), Delft, The Netherlands, 17–19 June 2020.
21. El Ouardi, H.; El Gadari, A.; Ounejjar, Y.; Al-Haddad, K. Conception and experimental validation of a standalone photovoltaic system using the SUPC5 multilevel inverter. *Electronics* **2022**, *11*, 2779. [[CrossRef](#)]
22. El Ouardi, H.; Alaoui ME, K.; Nabaoui, M.; Habib, M.; El Gadari, A.; Ounejjar, Y.; Kamal, A.H. Grid connected photovoltaic system based on SPUC5 inverter. In Proceedings of the 2021 22nd IEEE International Conference on Industrial Technology (ICIT), Valencia, Spain, 10–12 March 2021; Volume 1.
23. El Ouardi, H.; El Gadari, A.; Ounejjar, Y.; Al-Haddad, K.; Alibou, S. Grid connected Photovoltaic System Based on SPUC9 Inverter. In Proceedings of the 2020 5th International Conference on Renewable Energies for Developing Countries (REDEC), Marrakech, Morocco, 29–30 June 2020.

24. Siddique MA, B.; Khan, M.A.; Asad, A.; Rehman, A.U.; Asif, R.M.; Rehman, S.U. Maximum power point tracking with modified incremental conductance technique in grid-connected PV array. In Proceedings of the 2020 5th International Conference on Innovative Technologies in Intelligent Systems and Industrial Applications (CITISIA), Sydney, Australia, 25–27 November 2020; pp. 1–6.
25. Abou Jieb, Y.; Hossain, E.; Hossain, E. Solar Cell Properties and Design. In *Photovoltaic Systems*; Springer: Cham, Switzerland, 2022; pp. 57–71.
26. Ahmed, H.Y.; Abdel-Rahim, O.; Ali, Z.M. New High-Gain Transformerless DC/DC Boost Converter System. *Electronics* **2022**, *11*, 734. [[CrossRef](#)]

Disclaimer/Publisher’s Note: The statements, opinions and data contained in all publications are solely those of the individual author(s) and contributor(s) and not of MDPI and/or the editor(s). MDPI and/or the editor(s) disclaim responsibility for any injury to people or property resulting from any ideas, methods, instructions or products referred to in the content.